Published online 23 January 2017 *Nucleic Acids Research, 2017, Vol. 45, No. 5* **2283–2293**
doi: 10.1093/nar/gkx025

Reversible manipulation of the G-quadruplex structures and enzymatic reactions through supramolecular host–guest interactions

Tian Tian[1,†], Yanyan Song[1,†], Lai Wei[1,†], Jiaqi Wang[1], Boshi Fu[1], Zhiyong He[1], Xi-Ran Yang[2], Fan Wu[1], Guohua Xu[3], Si-Min Liu[2], Conggang Li[3], Shaoru Wang[1,*] and Xiang Zhou[1,*]

[1]College of Chemistry and Molecular Sciences, Institute of Advanced Studies, Key Laboratory of Biomedical Polymers of Ministry of Education, Wuhan University, Wuhan 430072, Hubei Province, China, [2]College of Chemical Engineering and Technology, Wuhan University of Science and Technology, Wuhan 430081, Hubei Province, China and [3]Wuhan Institute of Physics and Mathematics, Chinese Academy of Sciences, Wuhan 430071, Hubei Province, China

Received November 14, 2016; Revised January 03, 2017; Editorial Decision January 04, 2017; Accepted January 21, 2017

ABSTRACT

Supramolecular chemistry addresses intermolecular forces and consequently promises great flexibility and precision. Biological systems are often the inspirations for supramolecular research. The G-quadruplex (G4) belongs to one of the most important secondary structures in nucleic acids. Until recently, the supramolecular manipulation of the G4 has not been reported. The present study is the first to disclose a supramolecular switch for the reversible control of human telomere G4s. Moreover, this supramolecular switch has been successfully used to manipulate an enzymatic reaction. Using various methods, we show that cucurbit[7]uril preferably locks and encapsulates the positively charged piperidines of Razo through supramolecular interactions. They can switch the conformations of the DNA inhibitor between a flexible state and the rigid G4 and are therefore responsible for the reversible control of the thrombin activity. Thus, our findings open a promising route and exhibit potential applications in future studies of chemical biology.

INTRODUCTION

Supramolecular chemistry studies supramolecules, which are non-covalent association of complexes of two or more molecules (1–5). Consequently, it promises great flexibility and precision (6–8). The supramolecular reaction constitutes a powerful tool for constructing stimuli-responsive systems (9–11). As an underlying approach, supramolecular chemistry has been successfully used to fabricate functional nanoarchitectures and significantly contributes to the development of novel materials and applications (12). Supramolecular interactions are also deeply involved in the binding of substrates to active sites, transition state stabilization and catalysis (13). Therefore, their structural diversity and functional versatility show great potential for the reversible control of biological systems that are of particular significance (14,15), such as the structure of nucleic acids and enzyme regulation.

Nucleic acids can form a variety of three-dimensional structures through complex hydrogen bonds in different sequence contexts (16,17). Remarkably, guanine-rich repetitive sequences tend to fold into a four-stranded structure called a G-quadruplex (G4), which contains stacked planar G-quartets (shown in Supplementary Figure S1) (18). To date, it has been proven that a significant proportion of eukaryotic genomes can be converted into G4 structures (19), which were even visualized in human cells (20). In particular, the G4 is capable of adopting multiple conformations (21). Although G4 DNAs have been regulated by a variety of external stimuli (22,23), it remains a challenge to control these structures in a reversible manner. Recently, photo-induced conformational changes of nucleic acids have been achieved (24). We also reported the reversible light-control of a G4 structure using some azobenzene derivatives, such as Razo and Razo-s (structures shown in Supplementary Figure S2) (25,26). However, the major drawback of the photo-induced process is the depth limit of the excitation beam in tissues and biological systems. Therefore, it is important to develop new structure-switching strategies and we intend to utilize supramolecular interactions for this purpose.

*To whom correspondence should be addressed. Tel: +86 27 6875 6663; Fax: +86 27 6875 6663; Email: xzhou@whu.edu.cn
Correspondence may also be addressed to Shaoru Wang. Tel: +86 27 6875 6663; Fax: +86 27 6875 6663; Email: srwang@whu.edu.cn
†These authors contributed equally to the paper as first authors.

Recently, some significant advances have been made in developing supramolecular controllers (27). For example, a supramolecular switch has been reported that can reversibly control the antibacterial activity of specific molecules on demand (28). These synthetic systems usually depend on specific molecular recognition events between hosts and guests (29,30). Cucurbit[n]uril (CBn in Supplementary Figure S3), a multimeric macrocyclic and barrel-shaped molecule comprised of glycoluril rings and methylene bridges (31), represents an attractive host for supramolecular recognition due to its structural rigidity and ability to complex with a variety of guests (32). Of the known CBn homologues, CB7 (structure is shown in Supplementary Figure S3) has drawn particular attention because of its remarkable solubility in aqueous solutions (33,34). CB7 can bind to the guests with high biocompatibility and specificity. Importantly, it has been successfully used in many biological applications, such as fishing for plasma membrane proteins (35), regulation of bioorthogonal catalysis in cells (36) and the fabrication of biomimetic systems (37).

In the current study, supramolecular structure-switching of human telomere DNA (h-Telo in Supplementary Table S1) was first achieved in a reversible way (Figure 1A). Razo is capable of inducing the folding of flexible DNA into a rigid G4 structure (25). Upon adding CB7, the steric crowding associated with the non-covalent CB7-Razo complex prevents the approximation and contact of Razo with the DNA and therefore leads to a topological transition from G4 to the unfolded state (right-to-left direction in Figure 1A). Subsequently, the treatment with 1-Adamantanamine hydrochloride (AM in Supplementary Figure S3) disassembles the CB7–Razo interaction, due to the formation of a more stable complex between AM and CB7. The flexible DNA is then refolded into the rigid G4 structure again (left-to-right direction in Figure 1A). In striking contrast, CB7 does not appreciably interact with Razo-s (Figure 1B). UV-VIS titrations, Proton nuclear magnetic resonance (^{1}H-NMR) and molecular docking studies provide direct evidence that CB7 preferably locks and encapsulates the positively charged piperidines of Razo through host–guest interactions. More importantly, supramolecular switching of human telomere DNA has been successfully used to manipulate enzymatic reactions in a reversible and competitive manner. Thus, our findings open a promising route and exhibit potential applications in future studies of chemical biology.

MATERIALS AND METHODS

General methods and materials

The oligonucleotides were obtained from Invitrogen (Shanghai, China). Glycoluril (CAS# 496-46-8), sulfuric acid (CAS# 7664-93-9), formaldehyde solution (36.5–38% in H_2O, CAS# 50-00-0), acetone (CAS# 67-64-1), Adamantanamine hydrochloride (CAS# 665-66-7), KCl (CAS# 7447-40-7), Tris base (CAS# 77-86-1), Hydrochloric acid (CAS# 7647-01-0), Thrombin from human plasma (T6884) and Fibrinogen from human plasma (F3879) were obtained from Sigma-Aldrich Inc. (St. Louis, MO, USA). The CD experiments were performed on a Jasco-810 spectropolarimeter (Jasco, Easton, MD, USA) equipped with a Peltier temperature controller. The UV/VIS absorption spectra were recorded on a Shimadzu 2550 UV-VIS double-beam spectrophotometer. The ^{1}H nuclear magnetic resonance (NMR) spectra of the samples were determined at room temperature (RT) using a 300-MHz Varian Mercury-VX300 spectrometer. The light scattering intensity (LSI) of the sample was recorded using an LS55 fluorescence spectrometer (Perkin–Elmer Inc., USA) in the kinetics mode. The excitation and emission wavelengths were set at 650 and 650 nm, respectively. The detection was performed at RT with a 1-cm path-length cell.

Chemical synthesis

Compounds Razo, Razo-s and CB7 were synthesized according to the previous literatures (25,26,38).

Circular dichroism study

The circular dichroism (CD) spectra of the samples were collected using a Jasco-810 spectropolarimeter (Jasco, Easton, MD, USA) and a quartz cell (1-cm optical path length) at RT. CD spectra were collected from 200 to 340 nm at a scanning speed of 200 nm/min. The bandwidth was 5 nm and the response time was 2 s. All CD spectra were baseline-corrected for signal contributions from the buffer and were the average of at least two runs.

Supramolecular manipulation of the G4 structure

The representative process for deforming G4 is described below; h-Telo (10 μM) was dissolved in 1× assay buffer (10 mM Tris–HCl at pH 7.0), heated to 90°C for 4.0 min and then cooled slowly to RT. Subsequently, the newly synthesized ligand (either Razo or Razo-s) was added at a final concentration of 75 μM, and the mixture was incubated for 15 min at RT. The resulting sample was then treated with increasing concentrations (0–84 μM) of CB7 for 15 min and the CD spectra were determined and compared to a blank solution.

The representative process for reforming G4 is described below: the sample was prepared in 1× assay buffer containing 10 μM h-Telo, 75 μM ligand and 80 μM CB7. The following procedure is similar to the above one wherein AM is added sequentially to the starting preparation prior to measurement of the CD spectra.

UV-VIS titrations

The titrations were performed in 1× reaction buffer (10 mM Tris–HCl and 40 mM KCl, pH 7.0) at RT, with 20 μM ligand and the addition of increasing amounts (from 0 to 233 μM) of CB7, followed by a 10-min incubation. The spectrum of the sample was determined using a Shimadzu UV-2550 UV-VIS spectrophotometer with a quartz cell (1-cm path-length). The solution was excited at 340 nm, and the UV-VIS spectrum (area: 550–250 nm) was recorded at RT directly after the addition. The obtained spectra were zeroed at 550 nm. The results (full spectra as well as the plot of Abs@355 nm as a function of the concentration of CB7 added) were recorded. All spectra were baseline-corrected for the signal contributions from the buffer.

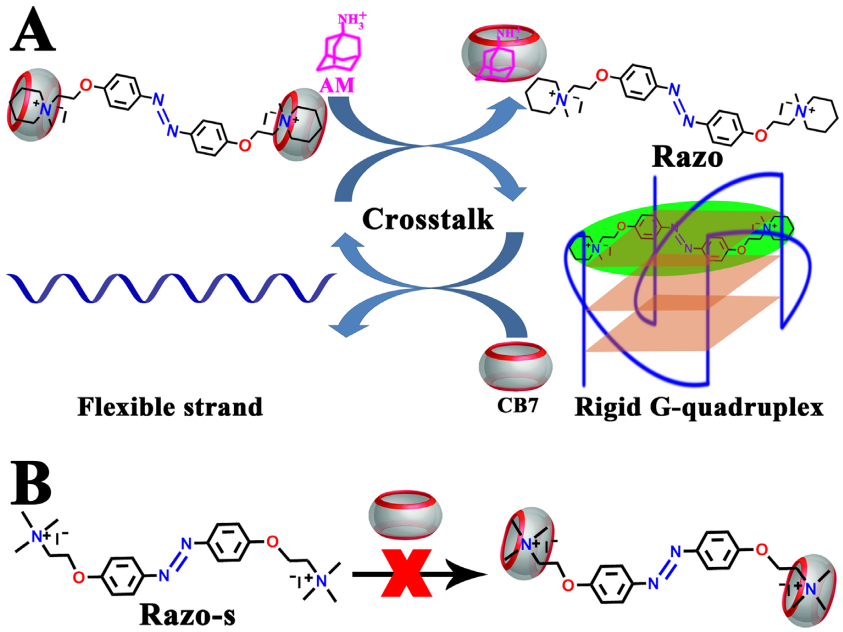

Figure 1. Schematic illustration of the design of the supramolecular switching of the G4 structure.

^{1}H-NMR assay

The ligand (0.005 mmol) was dissolved in 500 μl of d_6-DMSO at a final concentration of 10 mM and then analyzed. Next, CB7 solid (0.012 g, 0.01 mmol) was added to the above solution to obtain a suspension (CB7: ligand 2:1) that was stirred for 6 h at RT. Finally, the sample was centrifuged, and the supernatant of the mixture was collected and then analyzed. Next, AM (1.88 mg, 0.01 mmol) was added to the above CB7-Razo preparation and analyzed. The ^{1}H NMR spectrum of the sample was recorded at 298 K using a 300-MHz Varian Mercury-VX300 spectrometer. The signal assignments are based on the chemical shifts and intensity patterns. The MestReNova program was used to process the 1D-NMR spectrum obtained from the original data.

Molecular docking study

The aim of this study was to investigate the possible interactions between the ligand (Razo) and the receptor (CB7) when they were bound to each other. To obtain accurate results, all docking experiments were performed with the default parameters. The molecular structure of Razo was prepared and the Mulliken atomic charges were computed using density functional theory (DFT) calculations with the B3LYP functional and the 6–31G(d) basis set in Gaussian09 program (39,40). The geometry of Razo was optimized using the functional bp86 without geometry constraints and the lowest energy conformation was used for docking. The structure of the CB7 model was obtained from the deposited crystal structure of CB7 bound to insulin (Protein Data Bank Structure: 3Q6E) (41) and the charges were assigned by the Gasteiger-Hückel method (42). The Razo structure was then docked into the CB7 binding site using default procedure implemented in DOCK6 program (http://dock.compbio.ucsf.edu/DOCK_6/index.htm) with default parameters (43,44). This program uses the anchor and grows algorithm for flexible ligand docking. For docking, the box was generated using the CB7 binding site; the energetic grid was computed using the Grid module of the DOCK program with parameter file. The scoring in DOCK is based on the non-bonded terms of molecular mechanic force field.

Dock predicts the correct binding mode of ligand in the binding site of receptor. During docking, the receptor (CB7) was kept rigid and the ligand (Razo) was flexible. Snap binding energies were calculated and scored for each pose. Snap binding energy is the energy difference between the complex and the sum of the receptor and ligand energies. The poses were ranked according to the docking energy and geometry matching, and the top one (contact score of −184) was selected as the candidate. The final docked structure was fully optimized on the Gaussian09 software package using PM3MM method. The docking results were analyzed and visualized by using the ViewDock facility in UCSF Chimera package (http://www.cgl.ucsf.edu/chimera/) (45). Docking was performed on a Linux workstation (Ubuntu 14.04) with an Intel® Xeon® Processor E5-2640 (2.50 GHz) and 32 GB of RAM. UCSF Chimera was run on windows 10 equipped with an Intel® Core® Processor i5-4570 (3.20 GHz) and 32 GB of RAM.

Supramolecular manipulation of enzymatic reactions

This assay was performed according to previously reported protocols (46,47).

For this assay, human thrombin was prepared as a 0.10 U/ml solution in reaction buffer (10 mM Tris–HCl and 40 mM KCl, pH 7.0) and the activity of this sample was determined and used as a positive control. Next, Itelo (2.0 nM) was added to a new parallel thrombin sample (the same recipe as above) followed by a 15-min incubation and

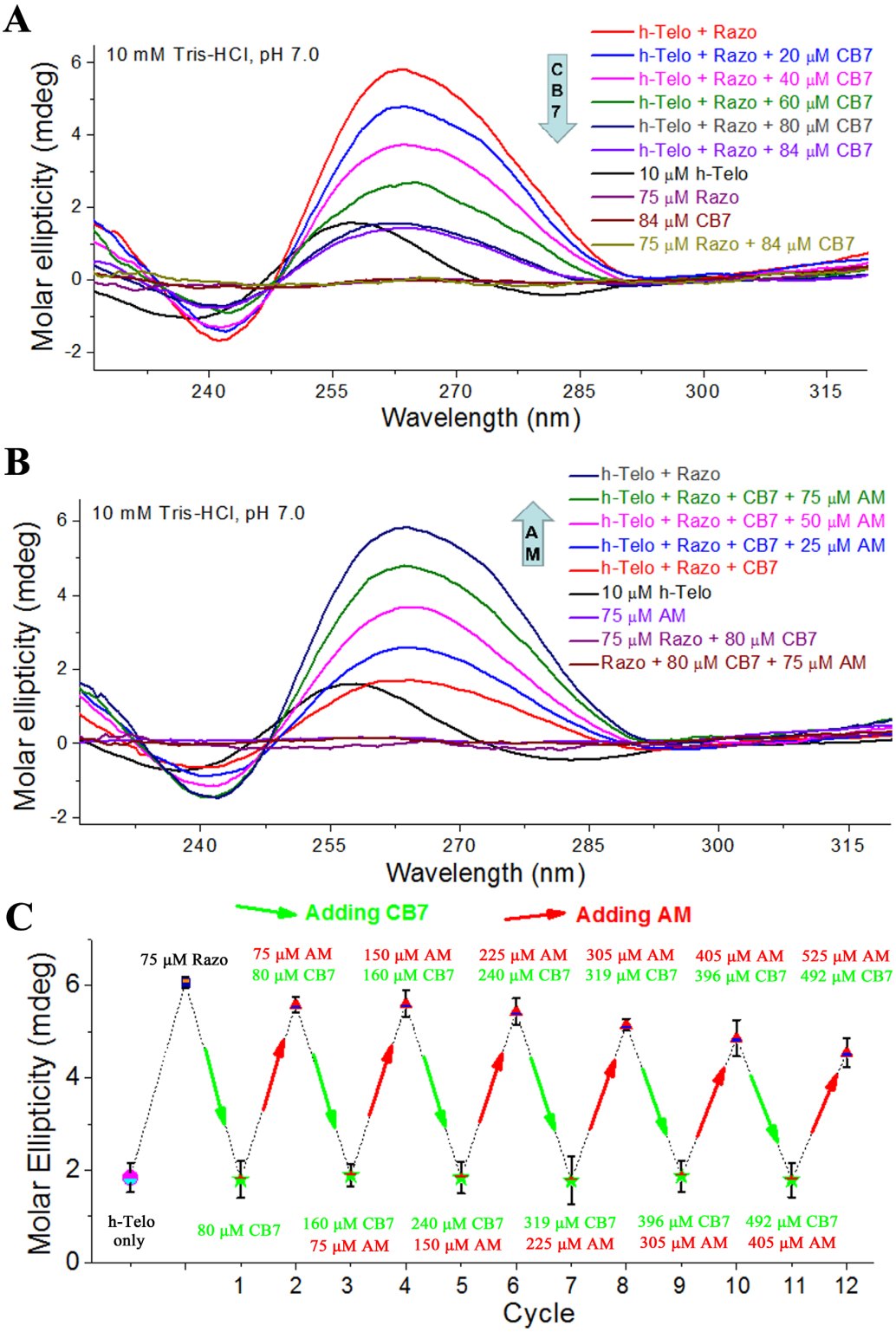

Figure 2. Supramolecular modulation of G4 Structures. (**A**) The influence of CB7 on the topological states of DNA. In this assay, the solution containing h-Telo (10 μM) was exposed to 75 μM Razo and then treated with increasing amounts of CB7. The arrow indicates the change in CD absorbance upon the addition of CB7. (**B**) The influence of AM on the topological states of DNA. In this assay, the solution containing h-Telo (10 μM), Razo (75 μM) and CB7 (80 μM) was prepared and subjected to increasing concentrations of AM. The arrow indicates the change in CD absorbance upon the addition of AM. (**C**) Repetitive supramolecular switching of G4 DNA between the 'on' and 'off' states. In this demonstration, the starting point indicates the CD absorbance of a 10 μM h-Telo solution at RT. Subsequently, Razo (75 μM) was added, and the resulting solution was subjected to CD measurements (second point). Subsequently, CB7 (green inset arrow) and AM (red inset arrow) were sequentially added to the same sample as indicated. After each addition, the solution was measured and the absorbance reading was shown in response to the input (the third to fourteenth points). All data are presented as the means ± SEM from three independent experiments. The error bars reflect the standard deviations.

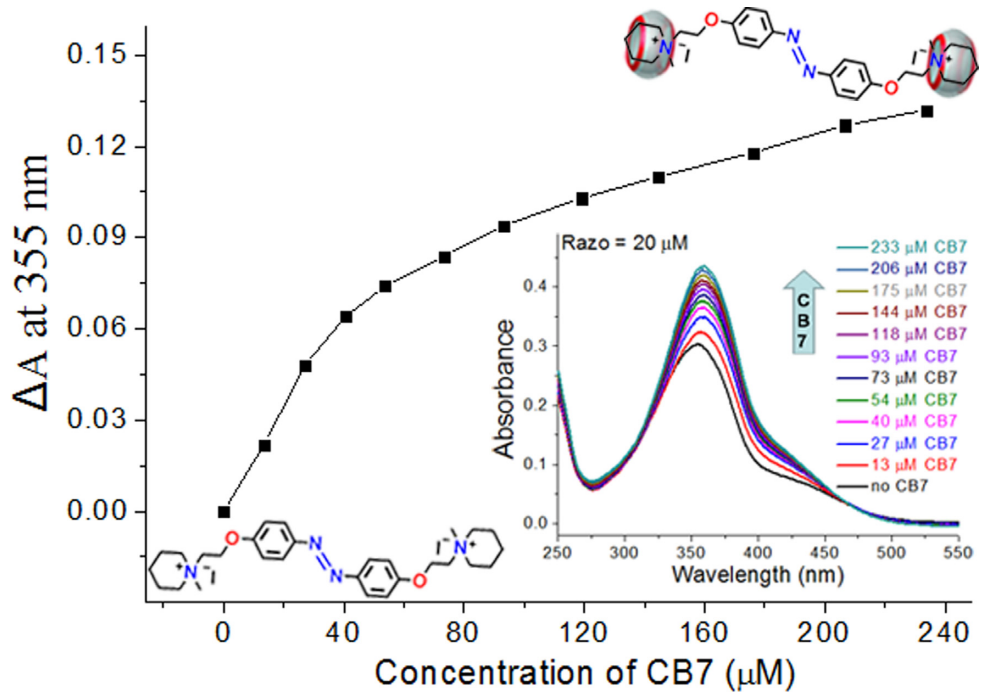

Figure 3. UV-VIS titration of Razo by CB7 in aqueous solution. The absorbance readings of Razo (20 μM) at 355 nm were plotted against the concentrations of added CB7 (0–233 μM). The insets show the corresponding UV-VIS spectral changes in Razo upon the addition of CB7.

the activity of this thrombin-Itelo sample was determined and used as a negative control. Subsequently, a new parallel thrombin-Itelo sample (the same recipe as above) was then treated with 65 μM Razo for 15 min and the activity of this thrombin-Itelo-Razo sample was examined.

For the CB7-induced inhibition assay, new parallel thrombin-Itelo-Razo samples (the same recipe as above) were then treated with various amounts of CB7 for 15 min and the activity was examined. For the AM-induced reactivation assay, the thrombin-Itelo-Razo-CB7 samples were treated with various amounts of AM for 15 min and the activity was examined.

The curve describing LSI versus time was measured using an LS55 fluorescence apparatus (Perkin–Elmer Inc., USA) in the kinetics mode at RT. The excitation and emission wavelengths were both set to 650 nm, and a 1-cm pathlength cell was used. Slit width: excitation = 10 nm; emission = 7 nm. For the kinetic measurements, 0.3 mg/ml fibrinogen was added at time (t) = 0. Untreated thrombin was used as an internal standard. All data were normalized to this control and expressed as a percentage.

Determining the effects of the regulator itself on the thrombin-fibrinogen reaction

The CB7 stock solution was prepared in aqueous solution. For this assay, human thrombin was prepared as 0.10 U /ml in the reaction buffer (10 mM Tris–HCl at pH 7.0, 40 mM KCl) and the activity of this sample was examined and used as a control. The regulator (CB7 or AM) was added to a new parallel thrombin sample (the same recipe as above) followed by a 15-min incubation and the activity of this thrombin-regulator sample was examined and normalized to the activity of the above control sample.

Statistical analysis

The statistical analysis was performed using the SPSS 19.0 software (SPSS Inc.). Differences were considered to be significant at $P < 0.05$.

RESULTS AND DISCUSSIONS

Design of the supramolecular switch

In the present study, we aim to develop a supramolecular switch capable of modulating DNA structures and enzymatic reactions. Appropriate operator molecules are required to achieve our goal. On the basis of our previous studies (25,26), Razo and Razo-s show excellent abilities to induce the formation of G4 structures and are therefore selected as the candidates. Molecular modeling studies indicate that the quaternary ammonium groups of Razo are deeply involved in the observed G4 binding (25). These bulky cations may fit into the CB7 cavity (28), thus preventing their access to the DNA phosphate backbone. Hence, CB7 is expected to serve as an 'OFF' switch for G4. As a positively charged and bulky compound, AM exhibits a high binding affinity (over 10^{12} M^{-1}) for CB7 (48), due to the good steric fit between ligand and receptor. Therefore, AM is expected to serve as an 'ON' switch for G4, due to its potential ability to remove the end-sealing units (CB7) from the cationic side-arms. Therefore, a plausible model of a supramolecular switch is designed to manipulate G4 structures.

Supramolecular modulation of G4 Structures

Razo and Razo-s were synthesized as previously reported (25,26). To prove the feasibility of our concept, h-Telo was tested as a model. CD is fast and allows comparative studies of DNA conformations in related conditions (21). The characteristic variations of CD spectra can reflect the conformational changes in DNA. As in our previous study (25,26), the addition of either Razo or Razo-s efficiently induced the conformational conversion of h-Telo from a single-stranded form into a parallel G4 structure, but there was no significant difference in the ability of these two molecules to induce G4 structures (Supplementary Figure S4). Then, we examined the influence of increasing amounts of CB7 on the topological states of h-Telo in the presence of G4 inducers. Importantly, Razo and Razo-s did fall into very distinct categories in response to CB7. The sequential addition of CB7 did not significantly influence the topology of h-Telo in the Razo-s sample, as reflected by the small changes in the shape and intensity of the CD bands (Supplementary Figure S5). In striking contrast to the Razo-s sample, the addition of CB7 decreased the band intensities of the Razo sample to a large extent, indicating that a large G4 deformation occurred (Figure 2A). Specifically, the treatment with 20 μM CB7 resulted in a significant decrease in the band intensity and this effect was more evident with the 40 and 60 μM treatments. Moreover, the treatment with 84 μM CB7 almost entirely diminished the Razo-mediated enhancement in CD absorption, indicating the nearly complete deformation of the G4. On the basis of these results, the behavioral differences between Razo and Razo-s might be attributed to the difference in their side-arms (Supplementary Figure S2). These findings raised an interesting possibility that CB7 specifically interacted with the positively charged piperidines of Razo, but not the N-trimethylethan-1-aminium moieties of Razo-s.

Having proved the efficient deformation of G4 under the influence of CB7, we anticipated that AM was able to generate active Razo and induce G4 reformation through supramolecular competition. To prove this point, increasing amounts of AM were added to the above preparation containing the two-component (Razo–CB7) system and further incubated before the CD spectra were measured. The representative data are shown in Figure 2B. Specifically, the treatment with 25 μM AM significantly enhanced the band intensity of the sample and this influence became more evident with the 50 μM treatment. Moreover, the 75 μM AM treatment largely diminished the CB7-driven deformation of G4 and the band intensity was very close to that observed for the Razo-treated sample. On the basis of these results, AM is able to relieve CB7-driven suppression of Razo-induced G4 formation in a dose-dependent manner.

An excellent switch should be able to withstand repeated stresses and sustain good reversibility over multiple cycles of treatments. To test the switching properties of our supramolecular assembly, h-Telo was subjected to the Razo treatment, followed by the sequential addition of the regulator (either CB7 or AM). After each addition, the mixture was incubated further before the CD spectra were collected. On the basis of our observations, the height of the CD band (Figure 2C) was significantly reduced by the excess CB7 relative to AM, and the observed spectrum (Supplementary Figure S6) has almost exactly the same shape as that of the DNA alone, indicating the efficient deformation of G4. Strikingly, the continual addition of AM produced an evident increase in the band intensity (Figure 2C and Supplementary Figure S6), indicating the switch to reformation of G4 by the presence of excess AM relative to CB7. Hence, this supramolecular switch can maintain reversible control of G4 by adjusting the concentrations of regulators on demand, which is indeed extremely easy to put into practice.

We next investigated whether the regulator itself (either CB7 or AM) was able to directly influence the DNA structure. The h-Telo sample was treated with various concentrations of the regulator in the presence or absence of 75 μM Razo. A high concentration (86 μM) of AM does not appear to markedly interfere with the parallel G4 structure induced by Razo (Supplementary Figure S7). Not surprisingly, the regulator treatment could not convert the flexible h-Telo into the parallel G4 structure, as reflected by the absence of the characteristic CD absorption (Supplementary Figure S8). These results clearly indicated that there was no direct interaction between the regulator and the different DNA structures. Therefore, the above structure-switching of DNA is attributable to supramolecular competition between Razo and AM for binding to CB7, but is not based on the interaction between the DNA and the regulator itself.

Study of supramolecular interactions

On the basis of the above results, it is reasonable to assume that supramolecular complexation between CB7 and Razo is responsible for the CB7-driven deformation of G4. To gain more insights into this behavior, UV-VIS titration of Razo with CB7 was performed in aqueous solutions (49). As shown in Figure 3, the UV profile of Razo reveals an absorption maximum near 355 nm (bottom line in inset image), which is the characteristic for a π–π* transition of a trans-azobenzene derivative (25). As CB7 was added, a gradual increase in the maximal absorption was observed, indicating weakened π–π stacking between the adjacent Razo chromophores (49). By further fitting the data to a 1:2 (guest:host) binding model (50,51), the binding constant of Razo with CB[7] was calculated to be 2.58×10^5 M^{-1}. This high value is often associated with the formation of a stable inclusion complex, which is primarily stabilized by strong host–guest interactions. Moreover, the sequential addition of AM to the Razo–CB7 preparation efficiently reduced the maximum absorption of the sample (Supplementary Figure S9). This expected phenomenon may indicate the disassembly of the CB7–Razo pair due to the formation of a more stable complex (AM-CB7). In striking contrast to the Razo results, much smaller changes in the maximum absorption were observed when Razo-s was titrated with increasing amounts of CB7 (Supplementary Figure S10). On the basis of these observations, it is concluded that Razo does indeed fit the CB7 cavity much better than Razo-s.

The ^{1}H-NMR analysis was performed to provide more direct evidence for the host–guest recognition between Razo and CB7. On the basis of the results (Supplementary Figures S11 and 12), the characteristic signals (7.0–8.0 ppm) of the aromatic protons in the Razo backbone were not obvi-

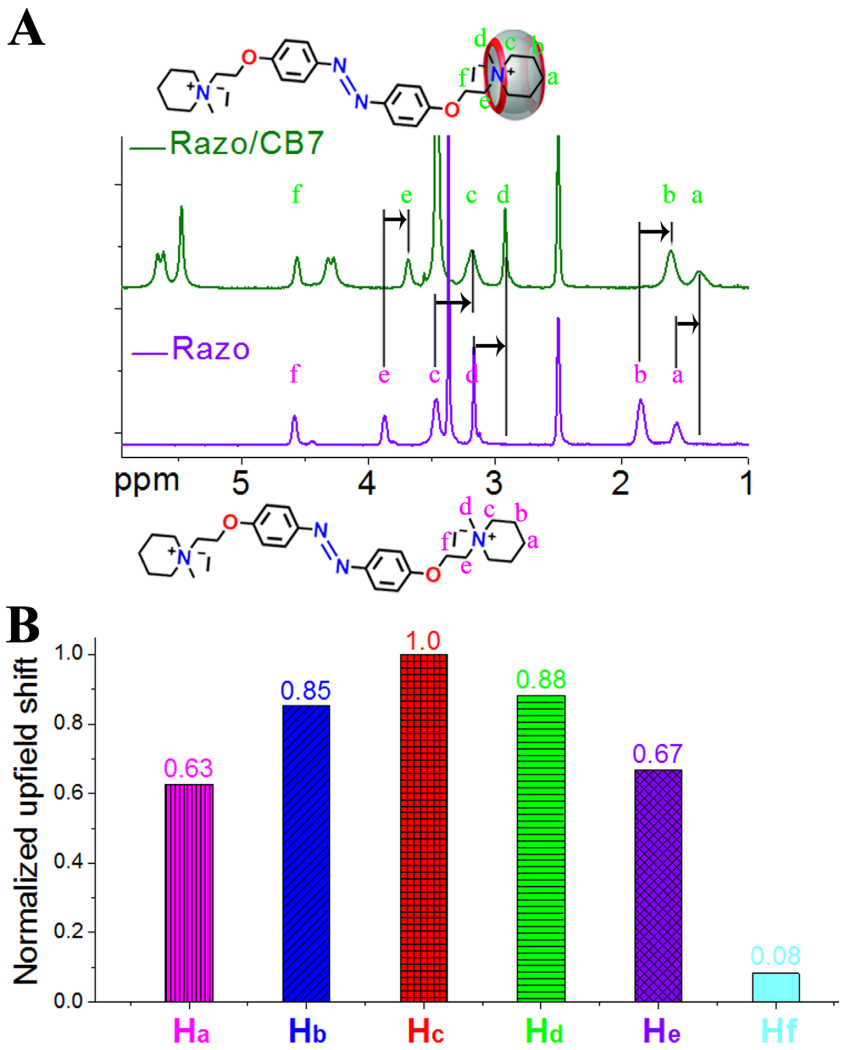

Figure 4. ^{1}H-NMR analysis of Razo before and after treatment with CB7. (**A**) The spectrum overlay of the selected region (δ = 5.9–1.0 ppm) is shown. All of the proton signals of CB7 were clearly detected upon the addition of CB7. All upfield peaks of Razo are labeled by letters (a–f), and their corresponding assignments are indicated in the appropriate place in the chemical structure (the bottom and top images). (**B**) The upfield shift value of each proton was normalized as a percentage relative to that of Hc.

ously shifted upon CB7 binding. This result provided evidence that the central aromatic unit was located outside the CB7 cavity (28). Figure 4A shows all upfield peaks of Razo in the absence (violet) and presence (dark green) of CB7. Importantly, this spectrum overlay indicates substantial upfield shifts in the proton peaks of free Razo that were ascribed to the positively charged piperidines (Ha, Hb, Hc and Hd in Figure 4A) at each end of the two side-arms. Such observed variations indicated shielding effects due to the inclusion of them into the CB7 cavity (49). For the -O-CH_2-CH_2-N- fragment of the bound Razo, an evident movement toward higher field (∼0.2 ppm) was detected for the two protons next to the nitrogen atom (He). However, there was almost no change in chemical shift for the other two protons next to the more electronegative oxygen atom (Hf). This phenomenon can be attributed to the fact that the methylene bridge (-CH_2-N-) of the bound Razo resides inside the macrocyclic host experience shielding effects, whereas the other methylene bridge (-O-CH_2-) was not included inside the shielding cavity.

Next, a detailed investigation of the NMR data was performed, and the corresponding assignments are listed in Supplementary Table S2. On the basis of these results, several important points can be identified. In particular, the largest upfield shift was observed for the N-CH_2- protons (Hc in Figure 4A and B) in the piperidine ring and considerably smaller changes in the shifts were observed for the protons (Hb and Hd) on vicinal neighboring carbons. For protons (Ha and He) exhibiting even longer distances to Hc, the upfield shifts are appreciably smaller than those for Hb and Hd. A sharp decrease in the upfield shift was observed for Hf. Therefore, it is concluded that the piperidine N-CH_2- of Razo preferably resides at the deepest position of the CB7 nanocavity. In a subsequent experiment, the addition of AM to the above preparation (Razo–CB7) resulted in downfield shifts of several identifiable protons (Hb, Hd and He in Supplementary Figure S13) to the unbound state, in-

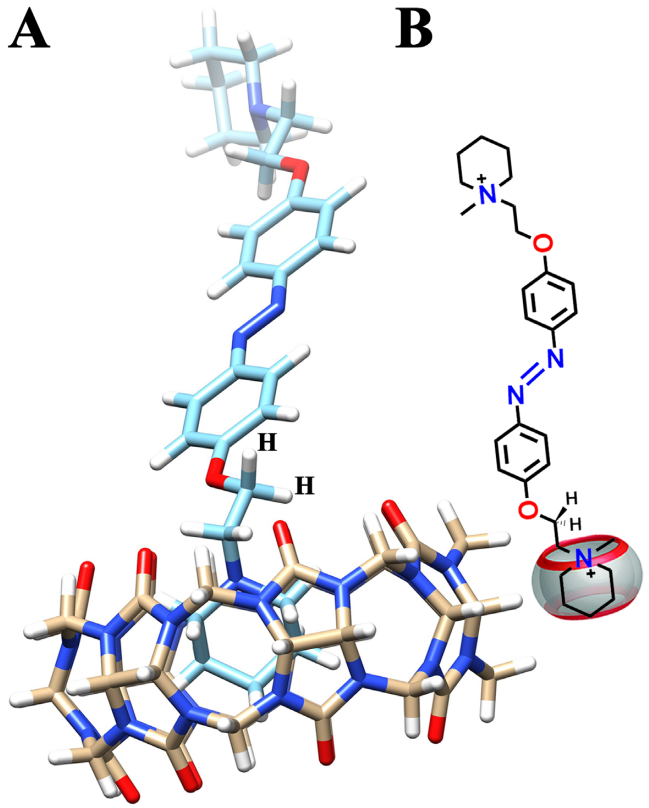

Figure 5. A side view of the optimized structure of the inclusion complex between Razo and CB7. (**A**) Razo is docked into the binding site of CB7, and the UCSF Chimera package is used to visualize the output. The methyl groups on the nitrogens and charges are omitted for clarity. The respective chemical elements are presented in different bright colors. The color scheme is: light blue for carbon (C); red for oxygen (O); sky blue for nitrogen (N); and white for hydrogen (H). (**B**) The corresponding structure of the Razo–CB7 complex.

dicating that specific decomplexation occurred. Moreover, the NMR signals of the Razo-s protons were not obviously influenced by CB7 treatment (Supplementary Figures S14, 15 and Table S3). These significant differences between Razo and Razo-s are consistent with those expected from the CD and UV-VIS results and therefore enhance the likelihood that the proposed host–guest interplay is responsible for the process by which G4 is manipulated.

Molecular docking study

Computational studies can complement experimental observations and further provide theoretical insights (52). Molecular docking has been widely used in the field of supramolecular chemistry (53) and was performed to predict the preferred orientation of Razo relative to CB7 when they were bound to each other. The 3D structure of CB7 was extracted from a deposited crystal structure of CB7 bound to insulin (PDB ID: 3Q6E) (41) and the charges were assigned using the Gasteiger-Hückel method (42). The Mulliken atomic charges of Razo were calculated using the DFT method with the Gaussian09 package (Supplementary Figure S16) (39). The optimized ligand conformation was then docked into the receptor molecule using the DOCK6 software such that the free energy of the overall system is minimized (43). Figure 5 shows the highest scoring model that illustrates the 'best-fit' orientation between Razo and CB7. Using this optimized model, it can be clearly observed that the cationic piperidine is completely buried inside the CB7 nanocavity. For the -O-CH_2-CH_2-N- fragment, the methylene bridge next to nitrogen atom (-CH_2-N-) resides very close to the electron-rich carbonyl portals of CB7 and thus it experiences high electron density in the inclusion complex. However, the methylene bridge next to oxygen atom (-O-CH_2-) observed in the complex protrudes outside the entrance to the shielding cavity of CB7. Therefore, the docking studies corroborate very well with the above NMR experimental results concluding that the CB7 ring locks the positively charged piperidines and gets stacked at each end of the side-arms.

Supramolecular manipulation of enzymatic reactions

Having shown the supramolecular basis for manipulating G4, we then pursued the translation of our discovery into practical applications, such as the reversible control of enzymatic reactions. To illustrate the proof-of-concept, a model system was established using the thrombin-fibrinogen reaction, which was determined using kinetic fluorescence assay (47). As in our previous study (46), the DNA-based inhibitor (Itelo in Figure 6A and Supplementary Table S1) was used. In the sequence of Itelo, two thrombin binding aptamers (15Apt and 29Apt) are connected by human telomere DNA (regulatory unit), which is allowed to change conformations upon treatment with CB7 or AM. Not surprisingly, thrombin was strongly inhibited by Itelo alone, and the activity was efficiently recovered after subsequent treatment with Razo. Importantly, the control assay indicated that the regulator (CB7 or AM) itself did not significantly affect thrombin in the presence or absence of Itelo (Supplementary Figures S17 and 18). We expect that CB7 can act as the trigger to induce the structural reshaping of Itelo and to deactivate the thrombin through molecular recognition with Razo (right-to-left direction in Figure 6A). To our delight, CB7 efficiently inhibited thrombin in a concentration-dependent manner (Figure 6B). Specifically, thrombin was obviously inhibited by the 20 μM CB7 treatment, and higher levels of inhibition were observed with the 30 and 40 μM treatments. Moreover, the 60 μM CB7 treatment almost completely abolished the reactivating effects of Razo. On the basis of these results, CB7 acts as a molecular brake to regulate thrombin activity in the multicomponent system.

On the basis of the ^{1}H-NMR and G4 reformation assay, the competitive inclusion of the AM molecule is able to drive the release of Razo from the CB7 cavity. Therefore, we anticipate that this event can lead to the reactivation of thrombin due to the binding of Razo to the G4 fragment and the resulting structural reorganization of Itelo (left-to-right direction in Figure 6A). Our strategic direction is fully supported by the following results, which showed a gradual recovery of thrombin activity in response to increasing amounts of AM (representative data are shown in Figure 6C). In particular, the 16 μM AM treatment resulted in an obvious recovery of the thrombin activity, and more than

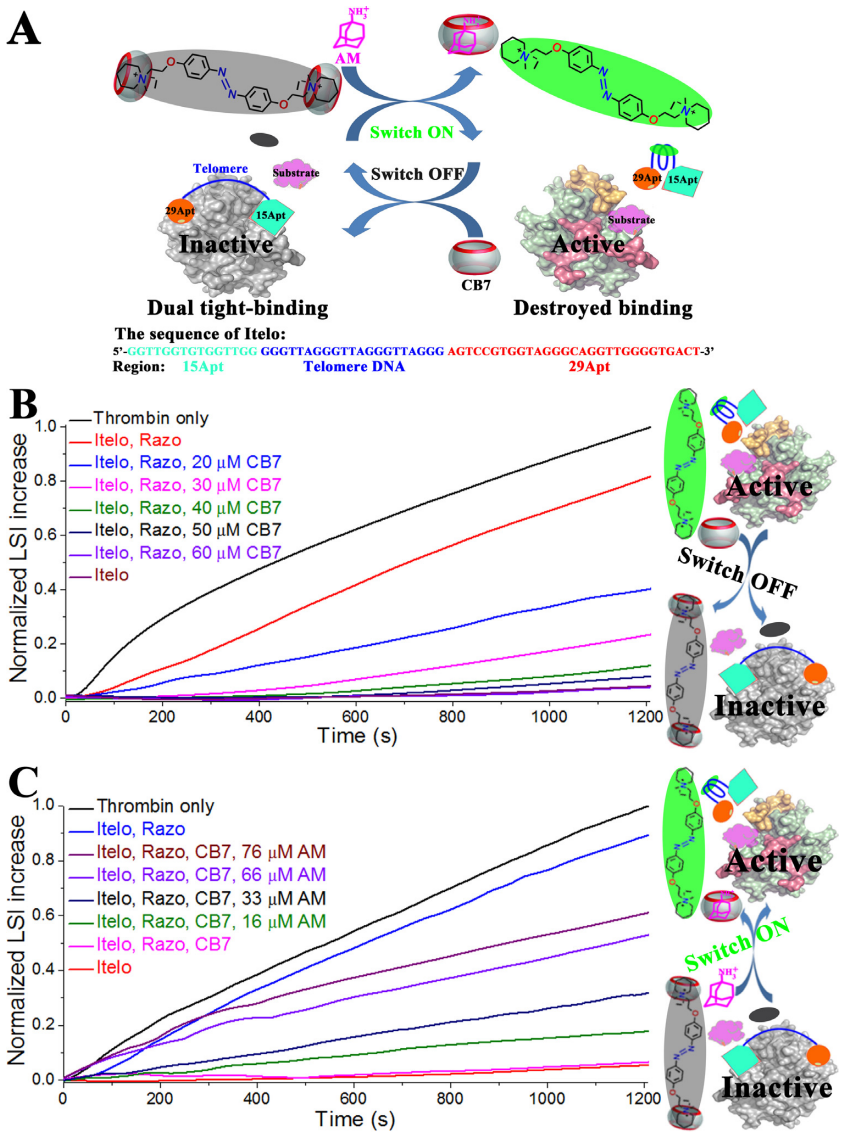

Figure 6. Supramolecular manipulation of enzymatic reactions. (**A**) Schematic illustration of the design and workflow. This supramolecular switch is based on the competition between Razo and AM for binding to CB7. (**B**) The influence of CB7 on the thrombin activities. Human thrombin (0.10 U/ml) was treated with the inhibitor Itelo (2.0 nM) and Razo (65 μM) and then treated with increasing amounts of CB7. The increase in LSI in the sample was normalized to that of the control sample (thrombin only). The arrow indicates the change in the thrombin activity upon CB7 treatment. (**C**) Reactivation efficacy of AM on the inhibited thrombin. The solution containing human thrombin (0.10 U/ml), the inhibitor Itelo (2.0 nM), Razo (65 μM) and CB7 (60 μM) was treated with increasing amounts of AM. The increase in LSI in the sample is normalized to that of the control sample (thrombin only). The arrow indicates the change in the thrombin activity upon AM treatment.

half of the enzyme activity was recovered upon treatment with 66 μM AM (Figure 6C). The control assay indicated that AM itself did not enhance the thrombin activity in the thrombin-Itelo-Razo system (Supplementary Figure S19). Not surprisingly, Razo-s can also recover the thrombin activity after inhibition, although a lower efficiency was observed compared to Razo (red and pink lines in Supplementary Figure S20, respectively). Consistent with the G4 switching assay, CB7 did not switch the thrombin from activation to inhibition in thrombin-Itelo-Razo-s system (blue line in Supplementary Figure S20). Together, these results indicate that AM acts as a molecular accelerator of thrombin activity through specific host–guest interactions in the multicomponent system.

DISCUSSION

Because the tertiary structure of nucleic acids plays a crucial role in the way they function, the development of a new structure-switching strategy has garnered much research interest (54,55). CB7 possesses a hydrophilic exterior and a hydrophobic cavity to encapsulate a variety of neutral or positively charged guests (56). Therefore, it has excellent potential to induce profound changes in the functional properties of these molecules. In the current study, a CB7-based molecular switch has been established utilizing supramolecular competition. UV-VIS titrations indicate that CB7 and Razo are able to form a stable complex, and AM can competitively disassemble this complex. As a result, the inter-

actions between Razo and DNA can readily break and reform, so that the DNA structures can be reversibly toggled between rigid (G4) and flexible (extended) states. The ^{1}H-NMR assay was performed to better understand the specific structural basis of this switch. On the basis of those results, the CB7 ring would likely encapsulate the positively charged piperidines of Razo to bring about evident changes in the corresponding proton signals, possibly due to excellent steric fit and electrostatic attractions between Razo's positively charged nitrogen atoms and the carbonyl groups in the CB7 outer rim. The molecular docking study shows the favorable conformation of Razo relative to the binding site of CB7 and further confirms the reliability of our experimental results.

Artificial regulation of enzymes can help researchers investigate and precisely control some important biological processes (57,58). In accord with the challenges, the findings from our group and others already revealed the potency of G4 architecture-based switches for this purpose (46,59). In the present study, supramolecular control of thrombin has been achieved by manipulating the interactions between Razo and G4 DNA. Thrombin is first exposed to Itelo, forming the inactive Itelo–thrombin complex. After treating the above system with Razo, the thrombin is released and activated through the formation of the Razo–Itelo complex. Subsequent treatment with CB7 shifts the thrombin from activation into inhibition, due to the switching process and formation of the CB7–Razo and Itelo–thrombin complexes. AM is able to initiate the cascade process to form the AM–CB7 and Razo–Itelo complexes and to release active thrombin. We concluded that the supramolecular switching of Razo between different states allows control of the global structure of Itelo and thus determines the catalytic activity of thrombin. Therefore, this supramolecular strategy offers a general and facile approach toward enzyme control.

CONCLUSION

In summary, the current study is the first to disclose a supramolecular switch for the reversible control of G4 structures. Moreover, it has been successfully used to manipulate an enzymatic reaction, which further shows the value of this switch. We believe that the newly developed strategy will serve as an useful tool and hold great promise in future biomedical applications.

SUPPLEMENTARY DATA

Supplementary Data are available at NAR Online.

ACKNOWLEDGEMENTS

We thank the large-scale instrument and equipment sharing foundation of Wuhan University.

FUNDING

National Basic Research Program of China (973 Program) [2012CB720600, 2012CB720603]; National Science Foundation of China [21432008, 91413109, 21672165, 21372182, 21572169]. Funding for open access charge: National Natural Science Foundation of China.

Conflict of interest statement. None declared.

REFERENCES

1. Wolf,K., Frahm,H. and Harms,H. (1937) The state of arrangement of molecules in liquids. *Z. Phys. Chem. Abt. B*, **36**, 237–287.
2. Lehn,J.M. (1990) Perspectives in supramolecular chemistry-from molecular recognition towards molecular information processing and self-organization. *Angew. Chem. Int. Ed. Engl.*, **29**, 1304–1319.
3. Zhang,Z., Kim,D.S., Lin,C.Y., Zhang,H., Lammer,A.D., Lynch,V.M., Popov,I., Miljanic,O.S., Anslyn,E.V. and Sessler,J.L. (2015) Expanded porphyrin-anion supramolecular assemblies: environmentally responsive sensors for organic solvents and anions. *J. Am. Chem. Soc.*, **137**, 7769–7774.
4. Liu,Z., Liu,G., Wu,Y., Cao,D., Sun,J., Schneebeli,S.T., Nassar,M.S., Mirkin,C.A. and Stoddart,J.F. (2014) Assembly of supramolecular nanotubes from molecular triangles and 1,2-dihalohydrocarbons. *J. Am. Chem. Soc.*, **136**, 16651–16660.
5. Cook,T.R., Zheng,Y.R. and Stang,P.J. (2013) Metal-organic frameworks and self-assembled supramolecular coordination complexes: comparing and contrasting the design, synthesis, and functionality of metal-organic materials. *Chem. Rev.*, **113**, 734–777.
6. Ma,X. and Zhao,Y. (2015) Biomedical applications of supramolecular systems based on host-guest interactions. *Chem. Rev.*, **115**, 7794–7839.
7. Zhou,Z., Yan,X., Cook,T.R., Saha,M.L. and Stang,P.J. (2016) Engineering functionalization in a supramolecular polymer: hierarchical self-organization of triply orthogonal non-covalent interactions on a supramolecular coordination complex platform. *J. Am. Chem. Soc.*, **138**, 806–809.
8. Mattia,E. and Otto,S. (2015) Supramolecular systems chemistry. *Nat. Nanotechnol.*, **10**, 111–119.
9. Xue,M., Yang,Y., Chi,X., Yan,X. and Huang,F. (2015) Development of pseudorotaxanes and rotaxanes: from synthesis to stimuli-responsive motions to applications. *Chem. Rev.*, **115**, 7398–7501.
10. Isaacs,L. (2014) Stimuli responsive systems constructed using cucurbit[n]uril-type molecular containers. *Acc. Chem. Res.*, **47**, 2052–2062.
11. Yang,H., Yuan,B., Zhang,X. and Scherman,O.A. (2014) Supramolecular chemistry at interfaces: host-guest interactions for fabricating multifunctional biointerfaces. *Acc. Chem. Res.*, **47**, 2106–2115.
12. Sokkalingam,P., Shraberg,J., Rick,S.W. and Gibb,B.C. (2016) Binding hydrated anions with hydrophobic pockets. *J. Am. Chem. Soc.*, **138**, 48–51.
13. Raynal,M., Ballester,P., Vidal-Ferran,A. and van Leeuwen,P.W. (2014) Supramolecular catalysis. Part 1: non-covalent interactions as a tool for building and modifying homogeneous catalysts. *Chem. Soc. Rev.*, **43**, 1660–1733.
14. Kaifer,A.E. (2014) Toward reversible control of cucurbit[n]uril complexes. *Acc. Chem. Res.*, **47**, 2160–2167.
15. Busseron,E., Ruff,Y., Moulin,E. and Giuseppone,N. (2013) Supramolecular self-assemblies as functional nanomaterials. *Nanoscale*, **5**, 7098–7140.
16. Velagapudi,S.P., Gallo,S.M. and Disney,M.D. (2014) Sequence-based design of bioactive small molecules that target precursor microRNAs. *Nat. Chem. Biol.*, **10**, 291–297.
17. Kendrick,S., Akiyama,Y., Hecht,S.M. and Hurley,L.H. (2009) The i-motif in the bcl-2 P1 promoter forms an unexpectedly stable structure with a unique 8:5:7 loop folding pattern. *J. Am. Chem. Soc.*, **131**, 17667–17676.
18. Parkinson,G.N., Lee,M.P. and Neidle,S. (2002) Crystal structure of parallel quadruplexes from human telomeric DNA. *Nature*, **417**, 876–880.
19. Balasubramanian,S., Hurley,L.H. and Neidle,S. (2011) Targeting G-quadruplexes in gene promoters: a novel anticancer strategy? *Nat. Rev. Drug. Discov.*, **10**, 261–275.
20. Biffi,G., Tannahill,D., McCafferty,J. and Balasubramanian,S. (2013) Quantitative visualization of DNA G-quadruplex structures in human cells. *Nat. Chem.*, **5**, 182–186.
21. Chung,W.J., Heddi,B., Schmitt,E., Lim,K.W., Mechulam,Y. and Phan,A.T. (2015) Structure of a left-handed DNA G-quadruplex. *Proc. Natl. Acad. Sci. U.S.A.*, **112**, 2729–2733.

22. Zhao,A., Zhao,C., Ren,J. and Qu,X. (2016) Enantioselective targeting left-handed Z-G-quadruplex. *Chem. Commun. (Camb)*, **52**, 1365–1368.
23. Li,X.M., Zheng,K.W., Zhang,J.Y., Liu,H.H., He,Y.D., Yuan,B.F., Hao,Y.H. and Tan,Z. (2015) Guanine-vacancy-bearing G-quadruplexes responsive to guanine derivatives. *Proc. Natl. Acad. Sci. U.S.A.*, **112**, 14581–14586.
24. Kamiya,Y. and Asanuma,H. (2014) Light-driven DNA nanomachine with a photoresponsive molecular engine. *Acc. Chem. Res.*, **47**, 1663–1672.
25. Wang,X., Huang,J., Zhou,Y., Yan,S., Weng,X., Wu,X., Deng,M. and Zhou,X. (2010) Conformational switching of G-quadruplex DNA by photoregulation. *Angew. Chem. Int. Ed. Engl.*, **49**, 5305–5309.
26. Xing,X., Wang,X., Xu,L., Tai,Y., Dai,L., Zheng,X., Mao,W., Xu,X. and Zhou,X. (2011) Light-driven conformational regulation of human telomeric G-quadruplex DNA in physiological conditions. *Org. Biomol. Chem.*, **9**, 6639–6645.
27. Pijper,D., Jongejan,M.G., Meetsma,A. and Feringa,B.L. (2008) Light-controlled supramolecular helicity of a liquid crystalline phase using a helical polymer functionalized with a single chiroptical molecular switch. *J. Am. Chem. Soc.*, **130**, 4541–4552.
28. Bai,H., Yuan,H., Nie,C., Wang,B., Lv,F., Liu,L. and Wang,S. (2015) A supramolecular antibiotic switch for antibacterial regulation. *Angew. Chem. Int. Ed. Engl.*, **54**, 13208–13213.
29. Yamaguchi,H., Kobayashi,Y., Kobayashi,R., Takashima,Y., Hashidzume,A. and Harada,A. (2012) Photoswitchable gel assembly based on molecular recognition. *Nat. Commun.*, **3**, 603.
30. Sun,R., Xue,C., Ma,X., Gao,M., Tian,H. and Li,Q. (2013) Light-driven linear helical supramolecular polymer formed by molecular-recognition-directed self-assembly of bis(p-sulfonatocalix[4]arene) and pseudorotaxane. *J. Am. Chem. Soc.*, **135**, 5990–5993.
31. Barrow,S.J., Kasera,S., Rowland,M.J., del Barrio,J. and Scherman,O.A. (2015) Cucurbituril-based molecular recognition. *Chem. Rev.*, **115**, 12320–12406.
32. Liu,S., Ruspic,C., Mukhopadhyay,P., Chakrabarti,S., Zavalij,P.Y. and Isaacs,L. (2005) The cucurbit[n]uril family: prime components for self-sorting systems. *J. Am. Chem. Soc.*, **127**, 15959–15967.
33. Cao,L., Sekutor,M., Zavalij,P.Y., Mlinaric-Majerski,K., Glaser,R. and Isaacs,L. (2014) Cucurbit[7]urilguest pair with an attomolar dissociation constant. *Angew. Chem. Int. Ed. Engl.*, **53**, 988–993.
34. Tang,H., Fuentealba,D., Ko,Y.H., Selvapalam,N., Kim,K. and Bohne,C. (2011) Guest binding dynamics with cucurbit[7]uril in the presence of cations. *J. Am. Chem. Soc.*, **133**, 20623–20633.
35. Lee,D.W., Park,K.M., Banerjee,M., Ha,S.H., Lee,T., Suh,K., Paul,S., Jung,H., Kim,J., Selvapalam,N. *et al.* (2011) Supramolecular fishing for plasma membrane proteins using an ultrastable synthetic host-guest binding pair. *Nat. Chem.*, **3**, 154–159.
36. Tonga,G.Y., Jeong,Y., Duncan,B., Mizuhara,T., Mout,R., Das,R., Kim,S.T., Yeh,Y.C., Yan,B., Hou,S. *et al.* (2015) Supramolecular regulation of bioorthogonal catalysis in cells using nanoparticle-embedded transition metal catalysts. *Nat. Chem.*, **7**, 597–603.
37. Gong,B., Choi,B.K., Kim,J.Y., Shetty,D., Ko,Y.H., Selvapalam,N., Lee,N.K. and Kim,K. (2015) High affinity host-guest FRET pair for single-vesicle content-mixing assay: observation of flickering fusion events. *J. Am. Chem. Soc.*, **137**, 8908–8911.
38. Vinciguerra,B., Cao,L., Cannon,J.R., Zavalij,P.Y., Fenselau,C. and Isaacs,L. (2012) Synthesis and self-assembly processes of monofunctionalized cucurbit[7]uril. *J. Am. Chem. Soc.*, **134**, 13133–13140.
39. Champagne,B., Bulat,F.A., Yang,W., Bonness,S. and Kirtman,B. (2006) Density functional theory investigation of the polarizability and second hyperpolarizability of polydiacetylene and polybutatriene chains: treatment of exact exchange and role of correlation. *J. Chem. Phys.*, **125**, 194114.
40. Becke,A.D. (1993) Density-functional thermochemistry. III. The role of exact exchange. *J. Chem. Phys.*, **98**, 5648–5652.
41. Chinai,J.M., Taylor,A.B., Ryno,L.M., Hargreaves,N.D., Morris,C.A., Hart,P.J. and Urbach,A.R. (2011) Molecular recognition of insulin by a synthetic receptor. *J. Am. Chem. Soc.*, **133**, 8810–8813.
42. Gasteiger,J. and Marsili,M. (1978) A new model for calculating atomic charges in molecules. *Tetrahedron Lett.*, **19**, 3181–3184.
43. Ewing,T.J., Makino,S., Skillman,A.G. and Kuntz,I.D. (2001) DOCK 4.0: search strategies for automated molecular docking of flexible molecule databases. *J. Comput. Aided Mol. Des.*, **15**, 411–428.
44. Hollick,J.J., Rigoreau,L.J., Cano-Soumillac,C., Cockcroft,X., Curtin,N.J., Frigerio,M., Golding,B.T., Guiard,S., Hardcastle,I.R., Hickson,I. *et al.* (2007) Pyranone, thiopyranone, and pyridone inhibitors of phosphatidylinositol 3-kinase related kinases. Structure-activity relationships for DNA-dependent protein kinase inhibition, and identification of the first potent and selective inhibitor of the ataxia telangiectasia mutated kinase. *J. Med. Chem.*, **50**, 1958–1972.
45. Pettersen,E.F., Goddard,T.D., Huang,C.C., Couch,G.S., Greenblatt,D.M., Meng,E.C. and Ferrin,T.E. (2004) UCSF Chimera–a visualization system for exploratory research and analysis. *J. Comput. Chem.*, **25**, 1605–1612.
46. Tian,T., Song,Y., Wang,J., Fu,B., He,Z., Xu,X., Li,A., Zhou,X., Wang,S. and Zhou,X. (2016) Small-molecule-triggered and light-controlled reversible regulation of enzymatic activity. *J. Am. Chem. Soc.*, **138**, 955–961.
47. Wang,J., Wei,Y., Hu,X., Fang,Y.Y., Li,X., Liu,J., Wang,S. and Yuan,Q. (2015) Protein activity regulation: inhibition by closed-loop aptamer-based structures and restoration by near-IR stimulation. *J. Am. Chem. Soc.*, **137**, 10576–10584.
48. Shetty,D., Khedkar,J.K., Park,K.M. and Kim,K. (2015) Can we beat the biotin-avidin pair?: cucurbit[7]uril-based ultrahigh affinity host-guest complexes and their applications. *Chem. Soc. Rev.*, **44**, 8747–8761.
49. Jiao,Y., Liu,K., Wang,G., Wang,Y. and Zhang,X. (2015) Supramolecular free radicals: near-infrared organic materials with enhanced photothermal conversion. *Chem. Sci.*, **6**, 3975–3980.
50. Cao,L. and Isaacs,L. (2014) Absolute and relative binding affinity of cucurbit [7]uril towards a series of cationic guests. *Supramol. Chem.*, **26**, 251–258.
51. Thordarson,P. (2011) Determining association constants from titration experiments in supramolecular chemistry. *Chem. Soc. Rev.*, **40**, 1305–1323.
52. Christensen,A.S., Kubar,T., Cui,Q. and Elstner,M. (2016) Semiempirical quantum mechanical methods for noncovalent interactions for chemical and biochemical applications. *Chem. Rev.*, **116**, 5301–5337.
53. Smith,L.C., Leach,D.G., Blaylock,B.E., Ali,O.A. and Urbach,A.R. (2015) Sequence-specific, nanomolar peptide binding via cucurbit[8]uril-induced folding and inclusion of neighboring side chains. *J. Am. Chem. Soc.*, **137**, 3663–3669.
54. Nutiu,R. and Li,Y. (2003) Structure-switching signaling aptamers. *J. Am. Chem. Soc.*, **125**, 4771–4778.
55. Li,D., Song,S. and Fan,C. (2010) Target-responsive structural switching for nucleic acid-based sensors. *Acc. Chem. Res.*, **43**, 631–641.
56. Lee,J.W., Samal,S., Selvapalam,N., Kim,H.J. and Kim,K. (2003) Cucurbituril homologues and derivatives: new opportunities in supramolecular chemistry. *Acc. Chem. Res.*, **36**, 621–630.
57. Binschik,J., Zettler,J. and Mootz,H.D. (2011) Photocontrol of protein activity mediated by the cleavage reaction of a split intein. *Angew. Chem. Int. Ed. Engl.*, **50**, 3249–3252.
58. Broichhagen,J., Jurastow,I., Iwan,K., Kummer,W. and Trauner,D. (2014) Optical control of acetylcholinesterase with a tacrine switch. *Angew. Chem. Int. Ed. Engl.*, **53**, 7657–7660.
59. Kim,Y., Phillips,J.A., Liu,H., Kang,H. and Tan,W. (2009) Using photons to manipulate enzyme inhibition by an azobenzene-modified nucleic acid probe. *Proc. Natl. Acad. Sci. U.S.A.*, **106**, 6489–6494.